A study of transparent contact to vertical GaN-based light-emitting diodes

D. W. Kim, H. Y. Lee, G. Y. Yeom, and Y. J. Sung

Citation: Journal of Applied Physics **98**, 053102 (2005);
View online: https://doi.org/10.1063/1.2007850
View Table of Contents: http://aip.scitation.org/toc/jap/98/5
Published by the American Institute of Physics

JOURNAL OF APPLIED PHYSICS **98**, 053102 (2005)

A study of transparent contact to vertical GaN-based light-emitting diodes

D. W. Kim, H. Y. Lee, and G. Y. Yeom[a]
Department of Materials Science and Engineering, Sungkyunkwan University, 300 Chunchun, Jangan, Suwon, Gyeonggi, Korea 440-746

Y. J. Sung
M&D Laboratories, Samsung Advanced Institute of Technology, 14-1, Nongseo, Giheung, Yongin, Gyeonggi, Korea 449-901

(Received 10 November 2004; accepted 30 June 2005; published online 7 September 2005)

In this study, transparent indium tin oxide (ITO) deposited by sputtering was applied to laser lift-off (LLO) GaN-based vertical light-emitting diodes (VLEDs) and the electrical and optical properties of ITO films were measured as a function of annealing conditions. The measured minimum resistivity of ITO film was about $3.78 \times 10^{-4}\ \Omega\,\text{cm}$ and the measured optical transmittance at 460 nm was 96.8% after the annealing process. In this condition, about $1 \times 10^{-5}\ \Omega\,\text{cm}^2$ of ITO contact resistance to LLO *n*-GaN could be obtained. By applying the transparent ITO layer to the LLO GaN-based VLEDs, a significant decrease of the forward operating voltage from 3.3 to 3.8 V at 20 mA could be obtained. © *2005 American Institute of Physics*. [DOI: 10.1063/1.2007850]

INTRODUCTION

GaN-based optoelectronic devices such as light-emitting diodes (LEDs) in blue and ultraviolet wavelength regions have been studied intensively for the application to full color or white color outdoor LED display, LED lighting, backlight for liquid-crystal displays, highly dense memory device, etc.[1–6] For these various applications of the devices, the development of extremely bright GaN-based LEDs is prerequisite. Especially, backlights for colored screens in mobile appliances, automotive headlights, general lightings, etc., were regarded as important applications of white LEDs, and a number of researchers are making efforts to develop the highly bright white LEDs.[7,8] However, during the conventional GaN-based LED fabrication, the *p* contact is made by depositing metal layers on the *p*-GaN located at the top of GaN-based LED quantum well structure. These metal contacts are only partially transparent, therefore, the light emitted from the top of the devices is lowered, and which results in low light-emission efficiencies for conventional GaN-based LED devices.

Therefore, in these days, many attempts are made to develop low-resistance contact processes to *p*-GaN with transparent oxides to increase light emission from the top of the devices.[9–12] In addition, device structures or techniques such as flip chip, laser lift-off (LLO), etc., were applied to develop highly efficient and vertical LEDs (VLEDs).[13–15]

In this study, a transparent conductive oxide was used to *n*-GaN of a vertical GaN LED which has *n*-GaN on the top of the device and its optical and electrical properties were investigated. As the contact and a current spreading layer to *n*-GaN, ITO was used because it is a conducting material with the resistivity of $\sim 10^{-4}\ \Omega\,\text{cm}$ and the transmittance is higher than 80% at 460 nm of the blue wavelength region. In addition, due to the refraction index of ITO (1.8–2.0), the ITO layer can reduce the total internal reflection losses of the generated light in the semiconductor and due to the excellent optical and electrical properties, the ITO layer can be applied to the transparent contact of large chip LED devices.

EXPERIMENT

In this study, reverse GaN-based LED structured wafers prepared by a LLO process of conventional GaN LED quantum well wafers (*p*-GaN/multiple quantum well/*n*-GaN/sapphire) were used as the substrates. Before the LLO process, highly reflective thick metal contact was formed on the *p*-GaN side by depositing palladium (Pd) as a *p*-contact metal using an *e*-beam evaporator and depositing a support layer after annealing of *p*-contact metal. After the formation of the supporting layer, a LLO process was performed using a KrF excimer laser (248 nm). Actually, the LLO process is using the differences of the laser energy absorption in materials due to its energy band gap. In this experiment, the KrF laser energy irradiated through the transparent sapphire substrate is absorbed at the boundary between GaN and sapphire, and which causes the localized decomposition of GaN at the boundary to Ga and N. By the application of this LLO process, the GaN structure could be successfully separated from sapphire wafer completely at the boundary. Therefore, reverse GaN-based LED structured wafers (*n*-GaN/multiple quantum well/*p*-GaN/Pd/support layer) were formed. To obtain a planar surface on the device, the LLO wafers were etched using a BCl_3 inductively coupled plasma (ICP) until 1–1.5-μm-thick *n*-GaN was remained. To obtain a planar surface, the used ICP condition was 1400 W of 13.56-MHz rf power, −150 V of dc bias voltage, and 10 mTorr of BCl_3.

As the contact materials to *n*-GaN, a typical patterned 100-μm-diameter Ti/Al or nonpatterned ITO was used. ITO was used as a transparent current spreading *n*-contact material layer. A 100-nm-thick ITO films were deposited on the LLO *n*-type GaN ($N_d \sim 10^{17}/\text{m}^3$) and corning glass using a dc magnetron sputter deposition system at room temperature.

---

[a] Electronic mail: gyyeom@skku.edu

0021-8979/2005/98(5)/053102/4/$22.50

To deposit ITO, O_2/Ar gas mixtures composed of 1.25-SCCM (standard cubic centimeter per minute) O_2/48-SCCM Ar and 1.5-SCCM O_2/48-SCCM Ar were used at 5 mTorr. As the ITO sputtering target, a sintered mixture of 10-wt % SnO_2 and 90-wt % In_2O_3 was used and the applied dc power to a 5-cm radius ITO target was 200 W. With this condition, the deposition rate of the ITO film was about 1.1 nm/min. In addition, to optimize the electrical and optical properties of the deposited ITO, annealing was carried out in a tube furnace with N_2 ambient at 300 °C from 0 to 7.5 min.

Electrical and optical properties of the deposited ITO films such as resistivities and transmittance were measured using a four-point probe and UV spectrometry as a function of annealing time. Also, its contact resistances to the LLO *n*-GaN were measured by a HP4145B semiconductor parameter analyzer as a function of annealing condition. Contact properties were measured using the circular transmission line method (C-TLM) prepared by a photoresist lift-off process. Finally, the LLO GaN VLEDs with the patterned 100-μm diameter Ti/Al contacts or with nonpatterned blank ITO contacts were fabricated after a Cr/Au pad formation and the die separation of 300×300 μm^2, and its current-voltage (*I*-*V*) characteristics were inspected using a HP4145B semiconductor parameter analyzer.

RESULTS AND DISCUSSION

Figures 1(a) and 1(b) show the resistivities and transmittances of the ITO films measured by a four-point probe and UV spectrometry as a function of annealing time from 0 to 7.5 min. As shown in Fig. 1(a), the resistivity of the ITO film deposited with 1.25-SCCM O_2/48-SCCM Ar gas chemistry was decreased with increasing annealing time to 7.5 min, and the lowest resistivity of 3.78×10^{-4} Ω cm could be obtained for 7.5 min of annealing. In the case of the ITO film deposited with 1.5-SCCM O_2/48-SCCM Ar gas chemistry, the resistivity was decreased initially with increasing annealing time to 5 min, however, the further increase of annealing time increased the resistivity. In general, the resistivity of the ITO films is related to the electrons donated by ionized oxygen vacancies and impurities in the film.[16] Room-temperature deposited ITO contains Sn impurities and oxygen vacancies, however, they are not well ionized because the deposited ITO is in an amorphous state at room temperature. By annealing the deposited ITO, the crystallinity of ITO is increased and the resistivity is decreased by increasing annealing temperature and time. Therefore, it is believed that, at a fixed annealing temperature, the resistivities are decreased with annealing time by locating oxygen vacancies and Sn impurities to substitutional sites, therefore, by donating more electrons. However, as the annealing time is increased, oxygen is added to the film even in the N_2 environment by the partial pressure of oxygen existing in the N_2 environment and oxygen vacancies are reduced. The increase of the resistivity of the ITO films deposited with the higher oxygen containing Ar/O_2 gas mixture after 5 min appears related to the more significant decrease of oxygen vacancies in the films compared to the decrease of the resistivity by increasing the crystallinity of the films.

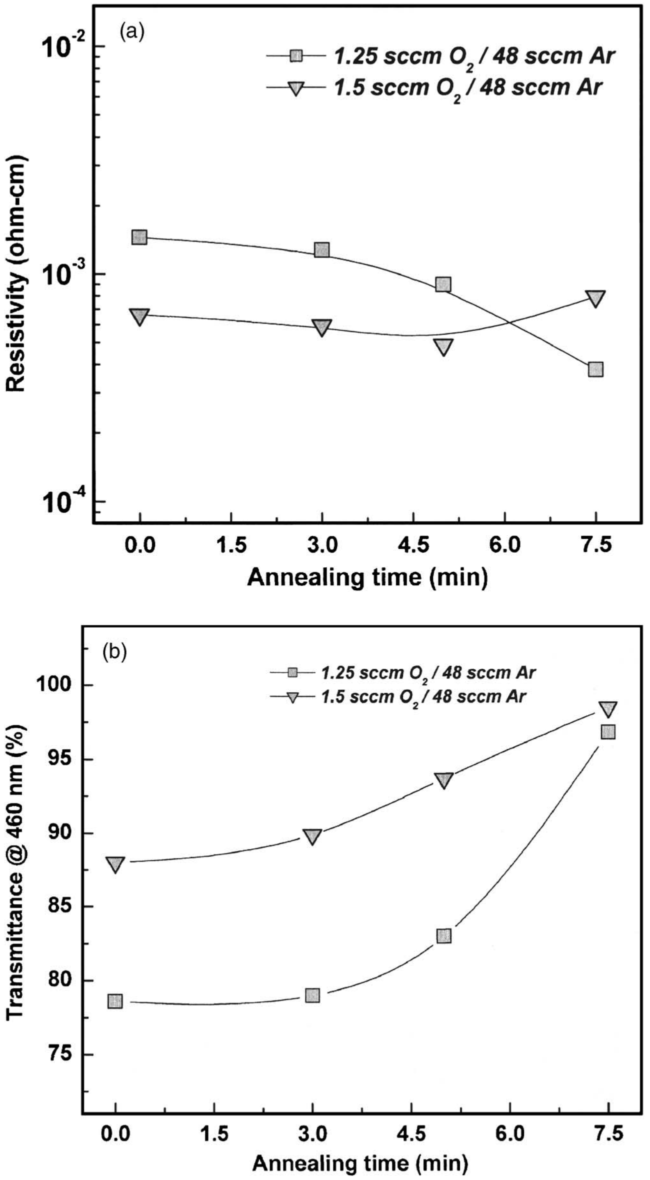

FIG. 1. The electrical and optical properties of ITO films as a function of annealing time. (a) The resistivities measured by a four-point probe and (b) the optical transmittance measured by UV spectrometry.

Figure 1(b) shows the measured optical transmittances of the ITO films as a function of annealing time. As shown in the figure, the increase of annealing time increased the optical transmittance of the ITO films. The transmittances at 460 nm for the ITO films deposited with 1.25-SCCM O_2/48-SCCM Ar and 1.5-SCCM O_2/48-SCCM Ar were increased from 78.6% to 96.8% and from 88% to 98.5% by annealing for 7.5 min, respectively, and the ITO films deposited with the higher oxygen contents showed the higher optical transmittance at a given annealing time. The increase of optical transmittance is related to the decrease of conducting electrons and the increase of ITO film's stoichiometry, therefore, it is related to the decrease of oxygen vacancies in the film by incorporating more oxygen in the film with increasing annealing time.

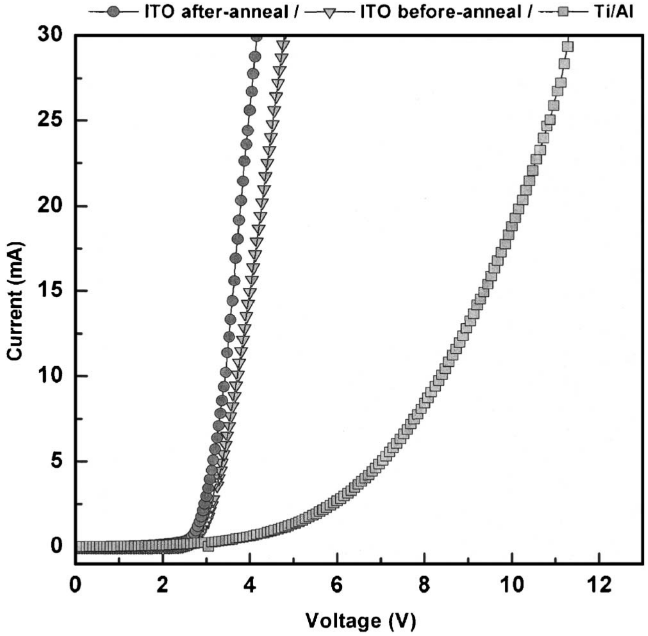

FIG. 2. *I-V* characteristic of LLO GaN VLEDs having *n*-GaN on the top of the devices with a Ti/Al contact and an ITO contact (before annealing and after annealing at 300 °C for 7.5 min after the deposition at room temperature).

Figure 2 shows the *I-V* curves of VLEDs with the 100-μm-diameter Ti/Al contacts and the deposited ITO contacts without patterning measured by the semiconductor parameter analyzer. As shown in the figure, the conventional Ti/Al contact applied to the LLO VLEDs showed a high operating forward voltage. The operating forward voltages of the fabricated devices with the Ti/Al contact at 20 mA were about 9–11 V. However, when the ITO was deposited to this device without patterning as a current spreading transparent contact layer instead of the patterned Ti/Al contact, the operating forward voltages of the devices were dramatically decreased to about 3.3–3.8 V for the ITO annealed for 7.5 min and about 4.0–4.4 V for the ITO before annealing. The high operating forward voltage for the typical *n*-GaN contact was not related to the Ti/Al contact resistivity. The Ti/Al contact resistivity to this LLO *n*-GaN was about $10^{-5}\ \Omega\ \text{cm}^2$ and the measured ITO contact resistivities to this LLO *n*-GaN were decreased from 8.5×10^{-5} to $1\times10^{-5}\ \Omega\ \text{cm}^2$ after annealing at 300 °C for 7.5 min in a N_2 ambient furnace.

To understand the high operating forward voltage for Ti/Al contact and the lowering of the voltage after ITO deposition for the LLO VLED, the schematic diagrams of the expected current paths of the LLO VLEDs for both contact structures were drawn in Fig. 3. In general, considering the voltage drop in vertical LEDs, if the current path "A" is followed, the total voltage drop (V_{total}) across from the *p* contact to the *n* contact can be written as

$$V_{\text{total-}A} = J(\rho_{p\ \text{contact}} + \rho_p t_p + \rho_n t_n + \rho_{n\ \text{contact}}) + V_a, \tag{1}$$

where the current density and voltage drop across the active region were represented as J and V_a, respectively. Also, $\rho_{p\ \text{contact}}$, ρ_p, ρ_n, and $\rho_{n\ \text{contact}}$ represented the resistivities of *p* contact, *p*-GaN, *n*-GaN, and *n* contact and t_p and t_n represented the thicknesses of *p*-GaN and *n*-GaN, respectively. The measured resistivity of the *n*-GaN exposed by the LLO process was about $4.2\times10^{-3}\ \Omega\ \text{cm}$ and appeared higher compared to that of the as-deposited *n*-GaN for the conventional lateral GaN possibly due to the diffusion of dopants during the following high-temperature deposition process for the device formation and possibly due to the loss of dopants during the LLO process even though the exact reason for the high resistivity of *n*-GaN needs further investigation. Also, the remaining *n*-GaN thickness was as thin as about 1–1.5 μm for the LLO VLED after the surface planarization process. Therefore, when a 100-μm-diameter Ti/Al contact was used as shown in Fig. 3(a), the high lateral current spreading resistance will be formed from the edge of contact pad to the edge of the device through the path "B" and its lateral spreading current path can be represented as l. Due to this resistance, the voltage drop for the path B will be as follows;

$$V_{\text{total-}B} = J(\rho_{p\ \text{contact}} + \rho_p t_p + \rho_n l + \rho_{n\ \text{contact}}) + V_a. \tag{2}$$

Therefore, the condition for the uniform current spreading will be as follows;

$$J\rho_n(t_n - l) \approx 0. \tag{3}$$

It can be obtained by increasing the thickness of *n*-GaN and it is the case for the conventional lateral GaN-based LED, where the thickness of the *n*-GaN is thicker than 3 μm and the resistivity is low enough. However, if the thickness of *n*-GaN (t_n) is increased, the voltage drop across the *n*-GaN region is increased by the resistivity of *n*-GaN (ρ_n). Therefore, the best way to minimize the additional voltage drop is to decrease the lateral current path (l) as much as the thickness of *n*-GaN (t_n). That is, the contact size must be increased as much as the device size or the effective current spreading length (l_e) of the *n*-GaN which indicates the effec-

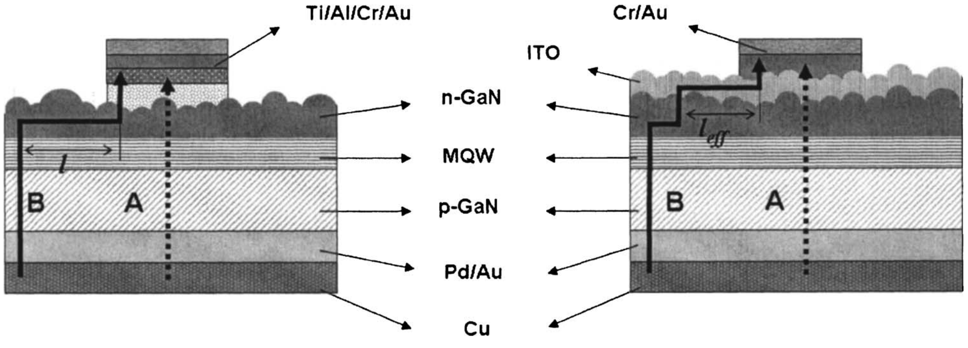

FIG. 3. Schematic diagram of the expected theoretical current paths of VLEDs. (a) The device with a Ti/Al contact and (b) the device with an ITO contact.

tively increased contact size from the edge of the contact metal should be increased by adding a current spreading layer on the semiconductor (n-GaN).[17]

By the deposition of a transparent conductive ITO layer as the current spreading layer on the top of n-GaN, as shown in Fig. 3(b), the voltage drop term in Eq. (2) by the lateral current path is changed from $J\rho_n l$ to $J[\rho_n(l-l_e)+\rho_{\mathrm{ITO}}l_e]$ and that by contact resistance is changed from $J\rho_{n\ \mathrm{contact}}$ to $J\rho_{\mathrm{ITO\ contact}}$, where the resistivity of the ITO layer was represented as ρ_{ITO} and the contact resistivity of the ITO to n-GaN as $\rho_{\mathrm{ITO\ contact}}$. If the contact resitivities are ignored due to the low contact resistivities, the differences of the voltage drop with and without the ITO contact for the path B can be estimated as

$$\Delta V \approx J l_e(\rho_n - \rho_{\mathrm{ITO}}). \tag{4}$$

The effective current spreading length (l_e) can be represented as a function of the resistivity (ρ_{cs}) and the thickness (t_{cs}) of the current spreading layer as follows;[17]

$$l_e = \mathrm{const}\sqrt{t_{\mathrm{cs}}/\rho_{\mathrm{cs}}}. \tag{5}$$

Therefore, the voltage drop shown in Eq. (4) can be rewritten as[17]

$$\Delta V \approx \mathrm{const}\, J\sqrt{t_{\mathrm{ITO}}/\rho_{\mathrm{ITO}}}(\rho_n - \rho_{\mathrm{ITO}}). \tag{6}$$

If the voltage difference shown in Eq. (6) is larger, the more uniform current spreading is obtained in the device shown in Fig. 3(b). It can be achieved by increasing the thickness of ITO layer and decreasing the resistivity of the ITO layer. Therefore, it can be seen that the improvement of electrical characteristics of the ITO contact device shown in Fig. 2 can be attributed to the improved lateral current spreading effect by the low resistivity of the deposited ITO layer.

CONCLUSIONS

In this study, the electrical and optical properties of ITO films as an application to the GaN LED current spreading contact were measured as a function of annealing time and their contact properties to LLO n-GaN were measured. The measured minimum resistivity of the ITO film was about $3.78\times10^{-4}\ \Omega\,\mathrm{cm}$ and the measured optical transmittance was 96.8% after annealing at 300 °C for 7.5 min. The transparent ITO contact was successfully applied to LLO GaN VLEDs having n-GaN on the top of the devices and the ITO contact layer is believed to play an important role in the high efficiency LLO GaN-based VLED fabrication by increasing the effective current spreading length.

ACKNOWLEDGMENT

This work was supported by the National Research Laboratory (NRL) Program of Ministry of Science and Technology in Korea.

[1] P. Schlotter, J. Baur, Ch. Hielscher, M. Kunzer, H. Obloh, R. Schmidt, J. Schneider, Mater. Sci. Eng., B **B59**, 390 (1999).

[2] U. Kaufmann *et al.*, Phys. Status Solidi A **188**, 143 (2001).

[3] V. Härle *et al.*, Phys. Status Solidi A **180**, 5 (2000).

[4] C. Huh, H. S. Kim, S. W. Kim, J. M. Lee, D. J. Kim, I. H. Lee, and S. J. Park, J. Appl. Phys. **87**, 4464 (2000).

[5] A. Motayed, A. V. Davydov, L. A. Bendersky, M. C. Wood, M. A. Derenge, D. F. Wang, K. A. Jones, and S. N. Mohammad, J. Appl. Phys. **92**, 5218 (2002).

[6] S. R. Jeon, Y. H. Song, H. J. Jang, G. M. Yang, S. W. Hwang, and S. J. Son, Appl. Phys. Lett. **78**, 3265 (2001).

[7] P. Schlotter, R. Schmidt, and J. Schneider, Appl. Phys. A: Mater. Sci. Process. **64**, 417 (1997).

[8] J. Baur *et al.*, Phys. Status Solidi A **194**, 399 (2002).

[9] Q. X. Yu, B. Xu, Q. H. Wu, Y. Liao, G. Z. Wang, R. C. Fang, H. Y. Lee, and C. T. Lee, Appl. Phys. Lett. **83**, 4713 (2003).

[10] R. H. Horng, D. S. Wuu, Y. C. Lien, and W. H. Lan, Appl. Phys. Lett. **79**, 2925 (2001).

[11] J. K. Sheu, Y. K. Su, G. C. Chi, M. J. Jou, C. C. Liu, and C. M. Chang, Solid-State Electron. **43**, 2081 (1999).

[12] S. J. Chang *et al.*, IEEE Photonics Technol. Lett. **16** 1002 (2004).

[13] A. Y. Kim *et al.*, Phys. Status Solidi A **188**, 15 (2001).

[14] Y. Kawakami, J. Shimadab, and S. Fujita, Proc. SPIE **4445**, 156 (2001).

[15] T. Fujii, Y. Gao, R. Sharma, E. L. Hu, S. P. DenBaars, and S. Nakamura, Appl. Phys. Lett. **84**, 855 (2004).

[16] Y. Wu, C. H. M. Marée, R. F. Haglund, Jr., J. D. Hamilton, M. A. Morales Paliza, M. B. Huang, L. C. Feldman, and R. A. Weller, J. Appl. Phys. **86**, 991 (1999).

[17] E. F. Schubert, *Light-Emitting Diode* (Cambridge University Press, Cambridge, UK, 2003).